World Journal of Surgical Oncology

RESEARCH

Open Access

SCNN1A expression in triple-negative breast cancer: clinical implications for prognosis and neoadjuvant therapy response

Xin Jin[1,2], Yue Ge[3], Tongjun Sun[3], Yunfei Ma[3], Yan Zhao[4,5,6], Qiang Xie[2], Faxiang Yin[2], Ligong Zhang[2] and Jun Qian[1,2*]

Abstract

Background This study aimed to identify differential genes between pathological complete response (pCR) and non-pCR following neoadjuvant chemotherapy in triple-negative breast cancer (TNBC). Additionally, the expression and clinical significance of the differential gene *SCNN1A* in TNBC were explored.

Methods Differential genes related to prognosis following neoadjuvant chemotherapy in TNBC were identified using the GEO database. Core genes were selected through the Cytoscape visualization and support vector machine (SVM) feature selection. The prognostic significance of these genes was assessed via online databases. *SCNN1A* expression and its correlation with clinicopathological data and neoadjuvant chemotherapy response were analyzed in 283 TNBC patients from the First Affiliated Hospital of Bengbu Medical University using immunohistochemistry.

Results Eleven core genes, including *SCNN1A*, were identified from 912 differential genes. High *SCNN1A* expression was associated with poor prognosis in TNBC patients via online database analysis. Gene set difference analysis (GSVA) and Gene set enrichment analysis (GSEA) revealed that *SCNN1A* was involved in several metabolic pathways. The clinical data indicated that high *SCNN1A* expression was associated with advanced T ($p=0.037$) and N stages ($p=0.011$), but not with age, HER2 status, Ki-67 expression, or histological grade. High *SCNN1A* expression was significantly more frequent in non-pCR patients compared to pCR patients, and high *SCNN1A* expression was associated with significantly lower overall survival (OS) and disease-free survival (DFS).

Conclusion *SCNN1A* overexpression is associated with poor prognosis and non-pCR status in TNBC patients undergoing neoadjuvant chemotherapy.

Keywords Triple-negative breast cancer, Neoadjuvant chemotherapy, GEO database, Immunohistochemistry, Survival analysis

*Correspondence:
Jun Qian
qianjun215036@sina.com
Full list of author information is available at the end of the article

Introduction

Breast cancer is the most common malignant tumor in women, and its incidence is steadily increasing, making it the leading cause of cancer-related death among women worldwide. Approximately 15% of all new cancer cases in women are attributed to breast cancer [1]. Triple-negative breast cancer (TNBC) is defined by the absence of estrogen receptor (ER), progesterone receptor (PR), and human epidermal growth factor receptor 2 (HER2) expression. TNBC accounts for about 15% to 20% of all breast cancer cases and is known for its high invasiveness, poor survival prognosis, and high incidence of recurrence and metastasis [2].

Advancements in gene chips and high-throughput next-generation sequencing (NGS) technologies have enabled researchers to exploit extensive gene databases within public repositories. In recent years, there has been a surge in the application of bioinformatics to mine microarray gene expression data. This has involved the analysis of differentially expressed genes that affect disease states and the identification of biomarkers for therapeutic intervention and prognostic assessment. Consequently, integrating gene expression data with bioinformatics methods offers a promising pathway to elucidate the pathogenesis of TNBC and identify potential therapeutic targets.

Material and methods

Gene expression profile data for 20 sample groups, comprising 10 samples each from the pathological complete response (pCR) group and the non-pathological complete response (non-pCR) group, were obtained by downloading the SeriesMatrixFile of dataset GSE25065. Differential expression between the pCR and non-pCR groups was analyzed by the limma package, with significant genes identified under a P-value < 0.05 and an absolute log fold change (|logFC|) > 1. Concurrently, raw mRNA expression data from the TCGA database to validate the findings. These differential genes were then introduced into the STRING online database to construct a protein–protein interaction (PPI) network. The top 100 genes were selected as key genes by Cytoscape for further analysis. The support vector machine (SVM) algorithm was utilized to select the tumor diagnostic markers, and the SVM-Recursive Feature Elimination (SVM-RFE) method, a machine learning technique that iteratively removes features to find the best variables, was applied to identify and evaluate characteristic genes in TNBC.

Using the SangerBox online analysis platform (http://vip.sangerbox.com/home.html), we analyzed the pan-cancer dataset to extract expression data for the *SCNN1A* gene across various samples, focusing specifically on breast cancer. Subsequently, the expression data of *SCNN1A* were analyzed to assess its prognostic significance in TNBC. This analysis was conducted using the KM Plotter tool (http://kmplot.com/analysis/) which processed mRNA-genechip data from the 203,453-at chip. Statistical significance was established at a p-value < 0.05.

The co-expression network of core genes was explored by correlation analysis based on the expression data from TNBC patients in the TCGA database. A filtering threshold for the correlation coefficient was set at 0.3, with a p-value < 0.05 considered statistically significant for establishing correlations. Visual representations of these correlations were generated using the "corrplot" and "circlize" packages, which facilitated the creation of correlation circle diagrams and heat maps, respectively.

Gene set difference analysis (GSVA) is a non-parametric, unsupervised method used to evaluate the enrichment of gene sets, translating gene-level changes into pathway-level changes. The gene sets were downloaded from the Molecular Signatures Database (MSigDB, version 7.0). Each gene set was comprehensively scored to evaluate the biological function changes in different samples. According to the expression of core genes, patients were categorized into high and low expression groups. The differences in signaling pathways between these groups were further analyzed by Gene set enrichment analysis (GSEA). The reference gene sets for this analysis were also obtained from the MSigDB. Pathway differential expressions between subtypes were analyzed, and significantly enriched gene sets were prioritized based on their consistency scores.

A total of 283 cases of TNBC were reviewed from the First Affiliated Hospital of Bengbu Medical University between January 2016 and June 2022. Among the patients, 48 underwent neoadjuvant chemotherapy, with 23 achieving pCR and 25 not achieving pCR. This study was approved by the Ethics Committee of Bengbu Medical University (2023YJS024). The relevant paraffin-embedded specimens and clinical data were collected from our hospital. All diagnoses of TNBC were confirmed by re-examination of the tissue blocks by at least two associate professors from the Department of Pathology. The medical records of the TNBC patients were reviewed, and telephone follow-ups were conducted to obtain information on the general condition of the patients, survival status, and other relevant data.

Immunohistochemistry

For immunohistochemical analysis, the SCNN1A antibody was sourced from Affinity Company. Additional reagents, including PBS buffer and DAB chromogenic solution, were acquired from Xiamen Haibiao Technology Co., Ltd (China). All specimens were fixed in 10% neutral-buffered formalin, embedded in paraffin, and

sectioned into 4 μm slices. The expression of SCNN1A was detected using the immunohistochemical Elivision method, following the manufacturer's instructions.

Standard for interpretation of immunohistochemical results

For immunohistochemical analysis, SCNN1A expression was assessed by observing its localization and staining intensity in the cytoplasm and on the cell membrane/serous. The cytoplasmic staining was characterized by brown particles indicating a positive reaction. High power microscopic observation was conducted in five randomly selected fields, with each field containing at least 200 cells.

The results were evaluated based on the proportion of positive stained cells and the intensity of staining. Staining intensity was graded as follows: 3 = strong brown expression, 2 = moderate brown expression, 1 = light yellow for weak expression, and 0 = no shading for non-expression. The extent of staining was categorized by the percentage of positive cells: < 5% = 0, 5%–25% = 1, 26%–50% = 2, 51%–75% = 3, and > 75% = 4. The final score was determined by multiplying the intensity grade by the extent category, with scores of 10–12 indicating strong positivity (+++), 6–9 moderate positivity (++), and 3–5 weak positivity (+). A score of ≥ 3 was considered positive, while a score < 3 was negative. Additionally, the overall positive rate was calculated.

Statistical methods

Clinical data were analyzed using SPSS software. The chi-square test and T-test were employed for univariate analyses to examine differences within categorical and continuous variables, respectively. The log-rank test was utilized to compare groups, specifically focusing on survival outcomes. Survival analysis was conducted using the Kaplan–Meier method.

Result

Differential gene analysis and core gene screening

The SeriesMatrixFile data file from the GSE25065 dataset was retrieved from the GEO public platform, identifying 912 differential genes, including 440 up-regulated and 472 down-regulated genes. A volcano plot was generated to visually represent these results (Fig. 1). Subsequently, the PPI network for these differential genes was accessed via the STRING online database (Fig. 2). Using Cytoscape software, the top 100 genes based on BETWEENNESS centrality were initially selected as key genes. To refine this selection, the SVM feature selection algorithm was employed to identify characteristic genes specific to TNBC, further evaluated using the SVM-RFE

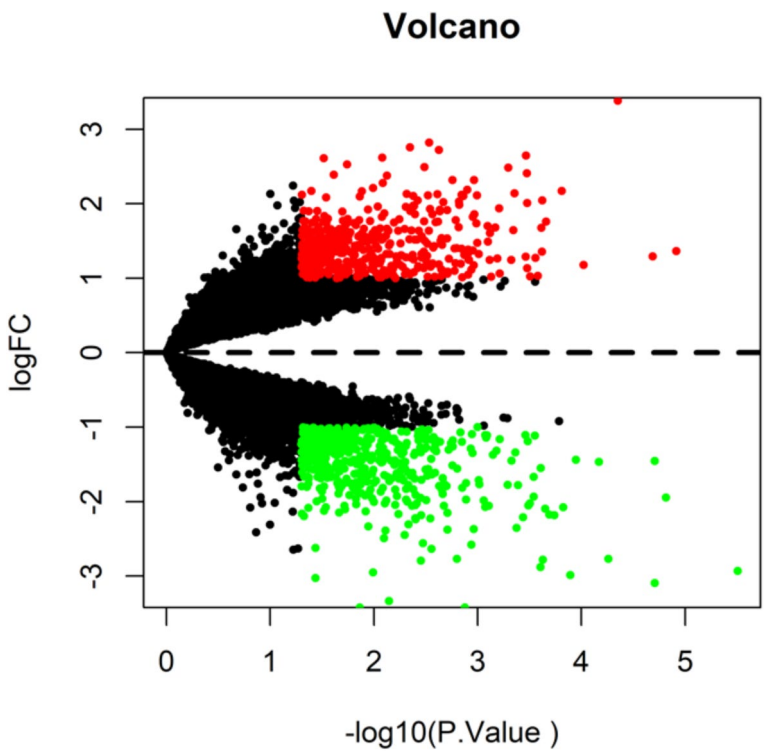

Fig. 1 Volcanic of differential genes

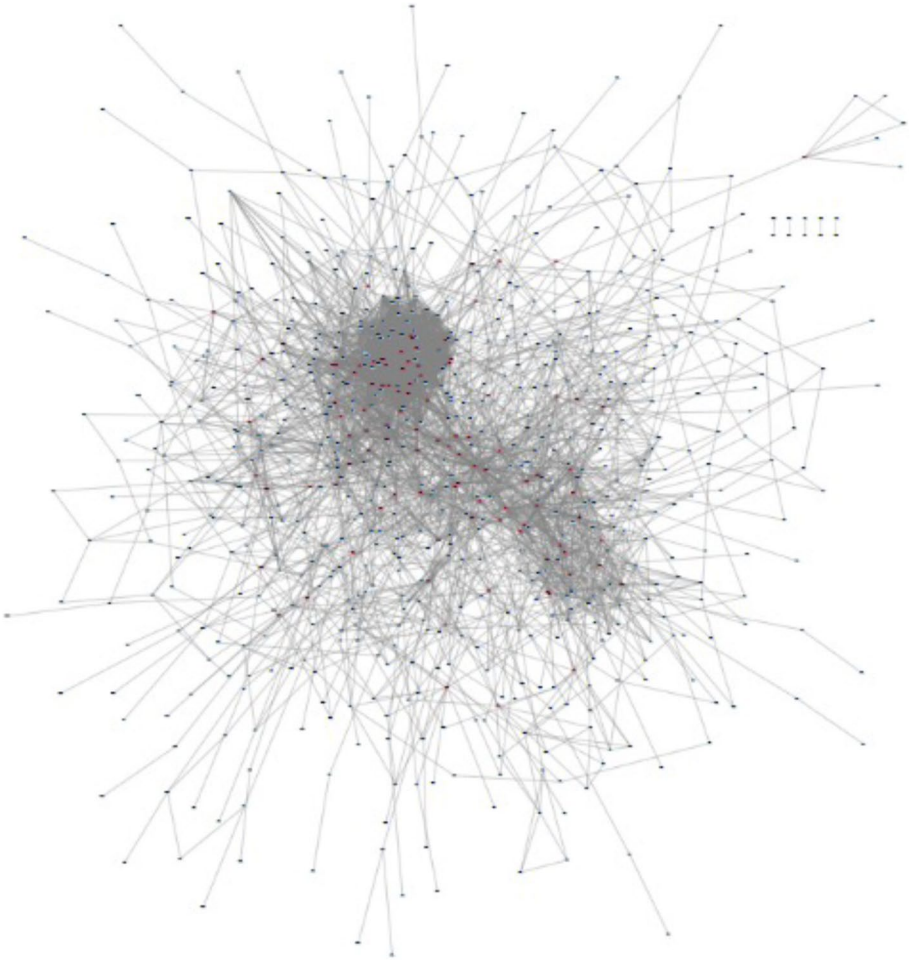

Fig. 2 PPI network protein

algorithm. This process resulted in the identification of 11 core genes—*MAPK3*, *OCA2*, *H2AFZ*, *CYP19A1*, *VPS39*, *STK11*, *SCNN1A*, *SMNDC1*, *UBE2D1*, *BSG*, and *HIVEP3*—through the intersection of the top 100 characteristic genes and the top 100 BETWEENNESS genes (Fig. 3).

Co-expression and pathway enrichment analysis of SCNN1A

The co-expression network of the *SCNN1A* gene was analyzed, identifying 456 motifs that exhibited a significant correlation with *SCNN1A* expression. The positively correlated genes included *MLPH*, *BCL2L1*, *FOXA1*, *PRR15*, *TSPAN1*, *DUSP5*, *SMIM14*, *PKIB*, *AC018629.1*, and *AGR3*, while negatively correlated genes included *TRIM65*, *E2F5*, *PAPSS1*, *POLR3G*, *VIM-AS1*, *MRPL15*, *LINC01956*, *SNHG16*, *SCARB1*, and *EN1* (Fig. 4). The heat map of top 10 positively and negatively correlated genes were generated (Fig. 5), and relationships were also visualized in a co-expression circle map (Fig. 6).

Pathway enrichment analyses using GSVA and GSEA revealed distinct signaling pathways associated with *SCNN1A* expression levels. GSVA indicated that high *SCNN1A* expression was predominantly associated with pathways like ESTROGEN RESPONSE EARLY, KRAS SIGNALING DN, and XENOBIOTIC METABOLISM. Conversely, lower *SCNN1A* expression correlated with enrichment in MYC TARGETS V2, MYC TARGETS V1, and UNFOLDED PROTEIN RESPONSE pathways (Fig. 7). In addition, GSEA results showed enrichment of *SCNN1A* in metabolic pathways, including Butanoate metabolism, Taurine and hypotaurine metabolism, and Tyrosine metabolism (Fig. 8).

Gene expression and prognostic analysis in TNBC

SCNN1A expression was analyzed across various cancer types using online databases, revealing a statistically significant higher expression in breast cancer tissues compared to normal tissue (Fig. 9). Focusing on TNBC, Kaplan–Meier survival analysis demonstrated that higher

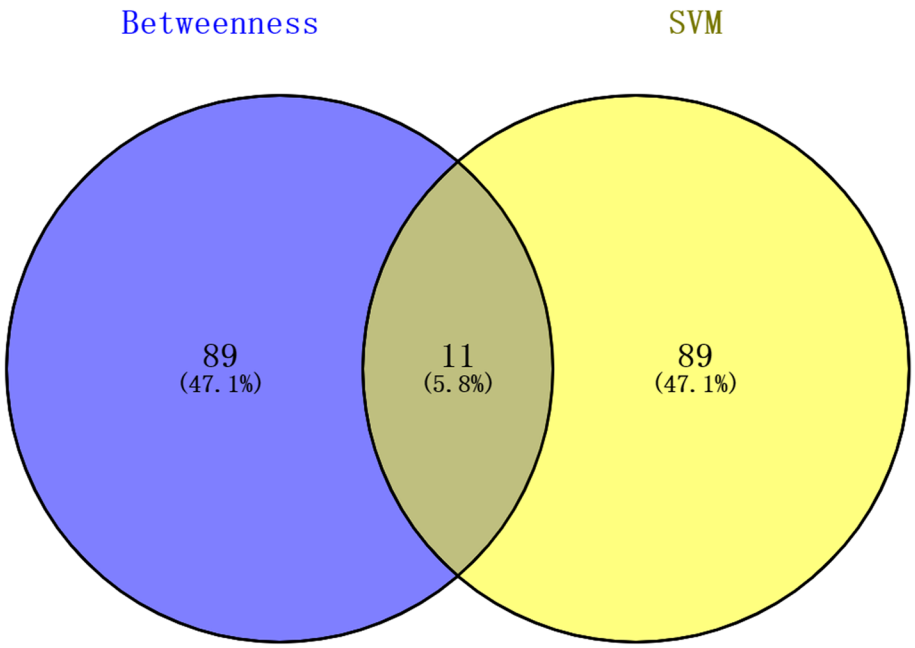

Fig. 3 screen the core genes

gene	cor	pvalue
MLPH	0.609	2.33E-10
BCL2L1	0.543	3.83E-08
FOXA1	0.535	6.50E-08
PRR15	0.533	7.35E-08
TSPAN1	0.53	9.44E-08
DUSP5	0.511	3.02E-07
SMIM14	0.501	5.76E-07
PKIB	0.498	6.90E-07
AC018629.1	0.492	9.83E-07
AGR3	0.489	1.14E-06

gene	cor	pvalue
TRIM65	-0.395	0.000126268
E2F5	-0.358	0.000579837
PAPSS1	-0.353	0.000685121
POLR3G	-0.349	0.000794884
VIM-AS1	-0.346	0.000909393
MRPL15	-0.345	0.000923585
LINC01956	-0.344	0.000951311
SNHG16	-0.339	0.001172063
SCARB1	-0.339	0.001170186
EN1	-0.337	0.0012283

Fig. 4 Correlation positive correlation gene

SCNN1A expression correlates with poorer prognosis, including overall survival (OS), recurrence-free survival (RFS), and distant metastasis-free survival (DMFS) (Fig. 10).

Clinicopathological data and correlation of SCNN1A expression

In this study, we analyzed paraffin-embedded tissue samples from 283 TNBC patients, among which 48 patients underwent neoadjuvant therapy (pCR, $n=23$; non-pCR, $n=25$). Patient demographics indicate that 155 patients were under 60 years old, while 128 were older than 60. Detailed clinicopathological characteristics are presented in Table 1.

Immunohistochemical staining revealed that SCNN1A was predominantly expressed in the cytoplasm, with strong staining observed in 151 cases (53.36%), indicating high expression, and weaker staining in 132 cases (46.64%), indicating low expression (Figs. 11 and 12). A significant association was found between high SCNN1A expression and advanced T stage ($p=0.037$) and N stage ($p=0.011$). However, no significant correlations were observed with age, HER2 status, Ki-67 index, or histological grade (Table 2).

Prognostic impact of SCNN1A expression in TNBC

Survival analysis was performed on 235 TNBC patients, excluding the 48 who completed standard neoadjuvant

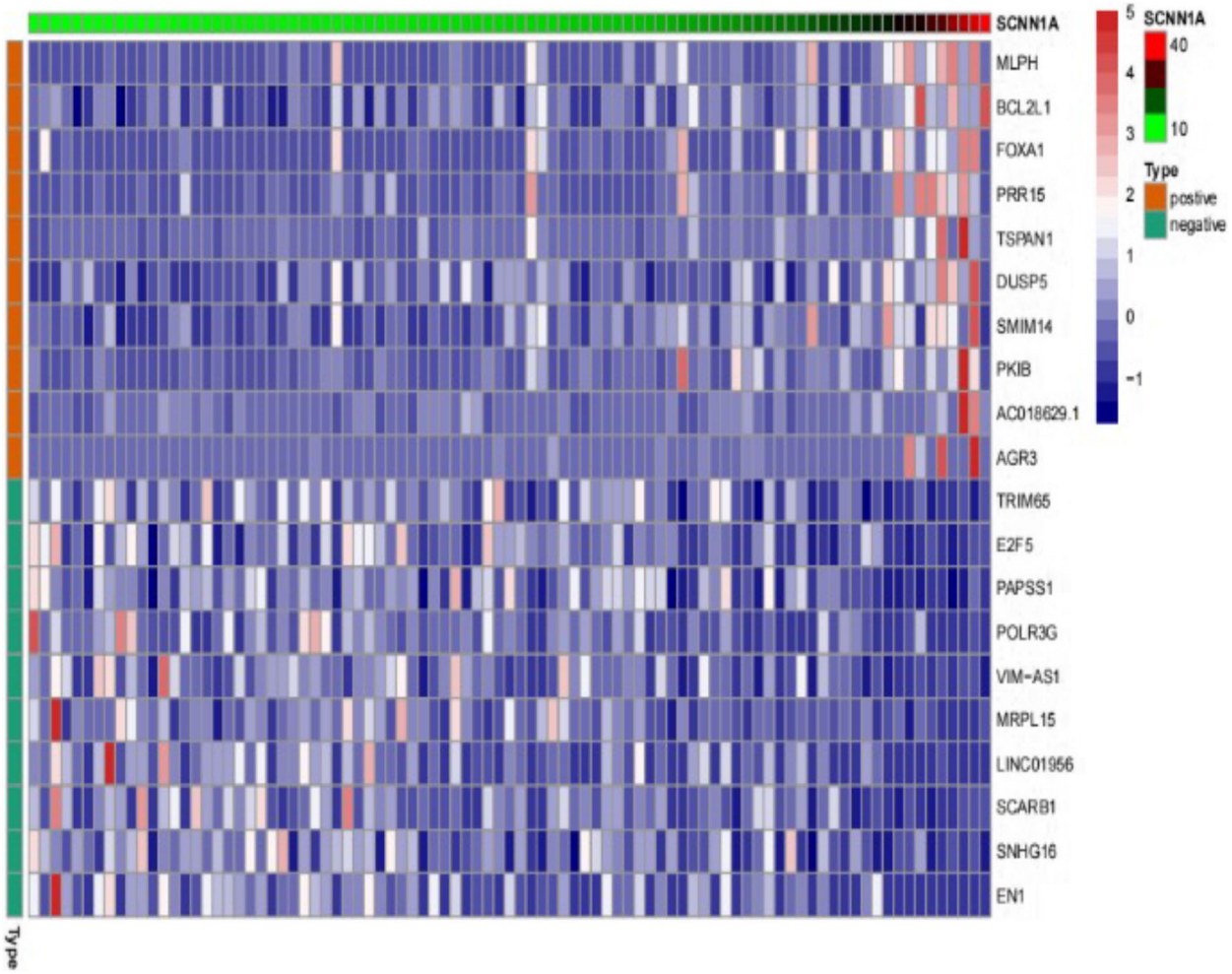

Fig. 5 Heat map of the correlated TOP10 genes with positive/negative correlation coefficients

therapy due to the short follow-up duration ranging from 4 to 22 months. The analysis revealed that patients with high expression of SCNN1A had a 5-year disease-free survival (DFS) rate of 58.33%, compared to 63.89% for those with low expression (Fig. 13). Similarly, the 5-year OS rates significantly differed, being 77.42% in patients with high expression versus 80.32% in those with low expression (Fig. 14).

Discussion

The three principal modalities for the treatment of malignant breast tumors are surgery, radiotherapy, and systemic chemotherapy, each of which presents unique advantages and challenges. It is well-recognized that curing breast cancer often requires more than a single treatment modality, leading to the common clinical approach of combination therapy to optimize therapeutic outcomes [3]. For patients with TNBC, chemotherapy and surgery remain the backbone of standard treatment. Some studies have demonstrated that higher expressions of TILs in patients with TNBC were associated with improved signifcantly DFS, OS, and pCR outcomes [4]. Despite the poor prognosis associated with TNBC, attributed to its aggressive biological behavior, these tumors frequently exhibit a relatively good response to chemotherapy, distinguishing them from other breast cancer subtypes. There has been a growing focus on targeted therapies for TNBC in recent years, driven by the urgent need to improve prognostic outcomes. Although TNBC lacks well-defined molecular targets, extensive research has identified signal pathway mutations post-neoadjuvant chemotherapy in many patients. These mutations present new opportunities for targeted interventions, which are currently under clinical investigation.

In this study, we utilized the GEO database to screen 912 differential genes from dataset GSE25065, which included 440 up-regulated and 472 down-regulated genes. Using Cytoscape, the top 100 key genes were

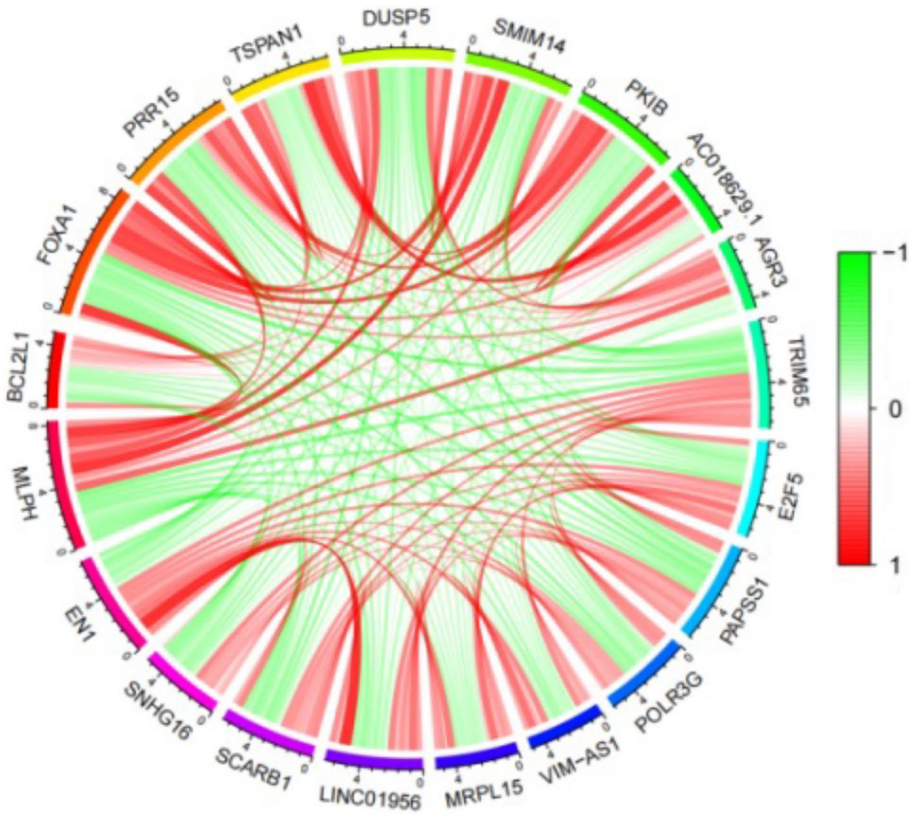

Fig. 6 Correlation coefficient positive/negative correlation TOP10 gene correlation circle

identified, and the SVM feature selection algorithm was applied to determine the top 100 characteristic genes. The intersection of these groups resulted in the identification of 11 core genes: *MAPK3*, *OCA2*, *H2AFZ*, *CYP19A1*, *VPS39*, *STK11*, *SCNN1A*, *SMNDC1*, *UBE2D1*, *BSG*, and *HIVEP3*. *SCNN1A* encodes a subunit of the epithelial sodium channel (ENaC), which is primarily expressed in epithelial tissue and functions as a sodium osmotic channel. Previous studies have highlighted the diverse roles of *SCNN1A* in various malignant tumors. For instance, both *SCNN1A* mRNA and protein levels of SCNN1A have been documented in ovarian cancer, where high expression of SCNN1A correlates with reduced OS and disease-specific survival (DSS), underscoring its association with poor prognosis in ovarian cancer [5]. Moreover, inhibition of *SCNN1A* has been shown to effectively curb proliferation, invasion, distant migration, and epithelial-mesenchymal transition (EMT) in pancreatic cancer cells [6]. Given these findings, our study aimed to explore the relationship between the expression of SCNN1A and prognosis in TNBC.

The co-expression analysis of the *SCNN1A* gene revealed 456 significantly expressed genes, with the *PKIB* gene in the TOP10 gene and positively correlated with *SCNN1A*. This suggests that *PKIB* may be involved in the pathogenesis of TNBC. PKIB, or CAMP-dependent protein kinase inhibitor β, is considered a regulator of CAMP-dependent protein kinase A signaling pathway. Triple-negative breast cancer is significantly related to the expression of PKIB. It is hypothesized that PKIB may modulate the Akt pathway by activating or phosphorylating Akt, thus promoting breast cancer progression via the Akt signal pathway [7]. Akt, a serine/threonine kinase, facilitates angiogenesis, cell growth, and proliferation and provides resistance against pro-apoptotic stimuli when activated or phosphorylated [8]. In various cancers, the Akt pathway is recognized as a crucial conduit for promoting invasive metastasis and has emerged as a promising target for cancer therapy [9]. Elevated phosphorylation levels of Akt are associated with poor prognosis in cancers [10]. Furthermore, studies have indicated that 17 β-estradiol can upregulate the expression and surface abundance of α-ENaC by activating the Akt signaling pathway and increasing phosphorylated Akt levels [11]. Given that *SCNN1A* encodes a subunit of the ENaC, and positively correlated with *PKIB*, it is plausible that *SCNN1A* may be implicated in the phosphorylation of Akt. Consequently, the positive correlation

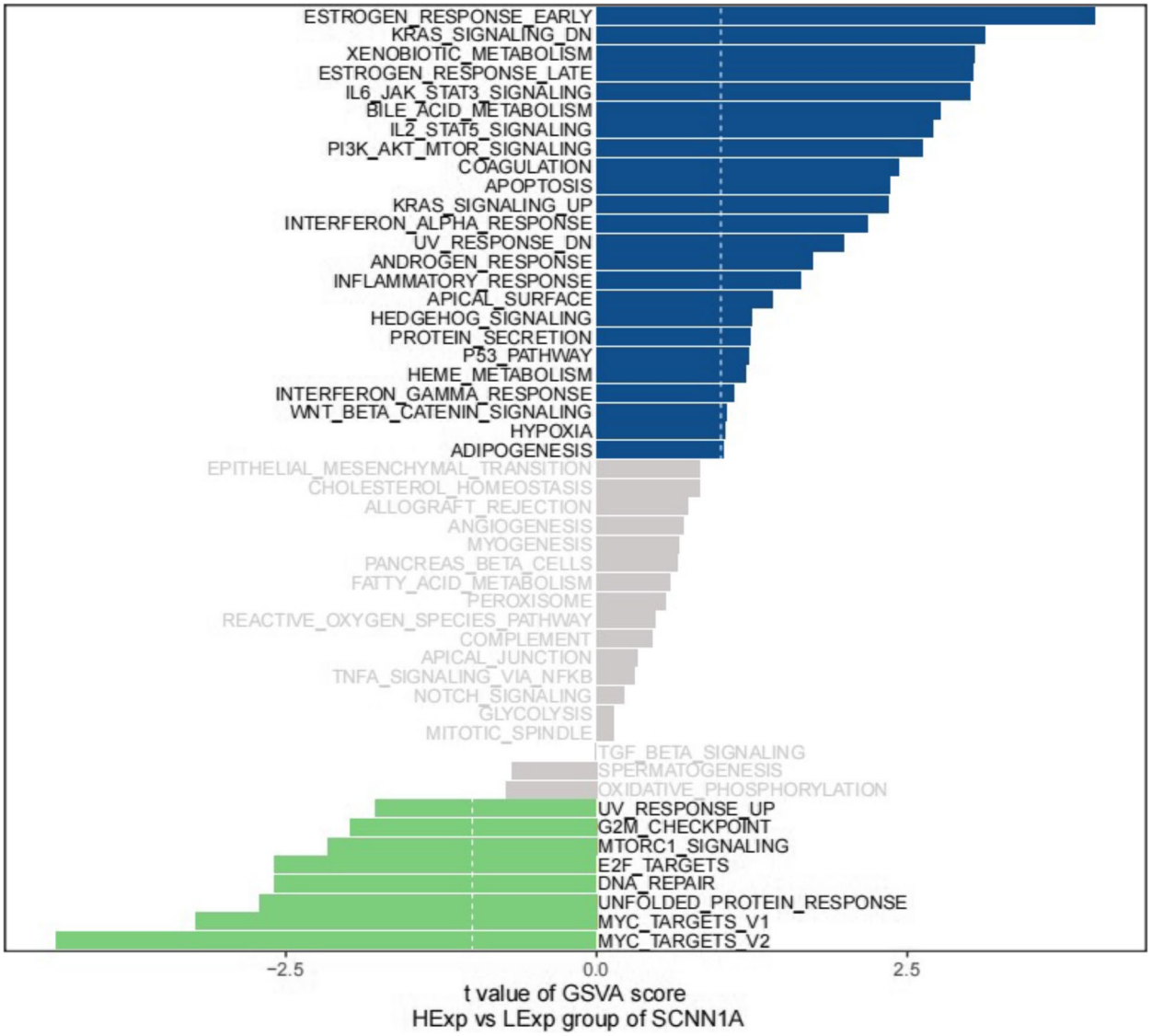

Fig. 7 Enrichment results of GSVA pathway of SCNN1A

between *SCNN1A* and *PKIB* suggests a potential mechanism underlying the onset and progression of TNBC, indicating both as potential targets for therapeutic intervention [12].

SCNN1A is located on chromosome 12p13.31 and forms part of a multi-subunit complex that comprises three subunits (α, β, and γ). *SCNN1A* specifically encodes α-subunit of ENaC, which is predominantly situated in the distal regions of kidney, distal colon, lung, and the epithelial tips of exocrine gland ducts. Each subunit of ENaC, including SCNN1A, SCNN1B, and SCNN1G, plays a critical role in sodium ion transport across the epithelium. Some studies have shown that sodium ions (Na^+) influx through ENaC promotes mitotic signaling and initiates the cell cycle. Inhibition of this sodium transport has been observed to reduce DNA synthesis necessary for cell proliferation. ENaC-mediated Na^+ influx enhances cancer cell proliferation, migration, and invasion [13]. Conversely, blocking Na^+ influx can trigger cell cycle arrest and induce apoptosis in cancer cells. This has been demonstrated in both in vitro and in vivo studies, where *SCNN1A* overexpression was shown to drive osteosarcoma tumor growth [14] and was implicated in the aggressive behaviors of ovarian cancer cells [15].

Additionally, ENaC-mediated Na^+ influx influences intracellular signaling pathways, such as the stabilization of GILZ1 via SGK1. GILZ1 inhibits the ubiquitination and subsequent proteasome-mediated degradation

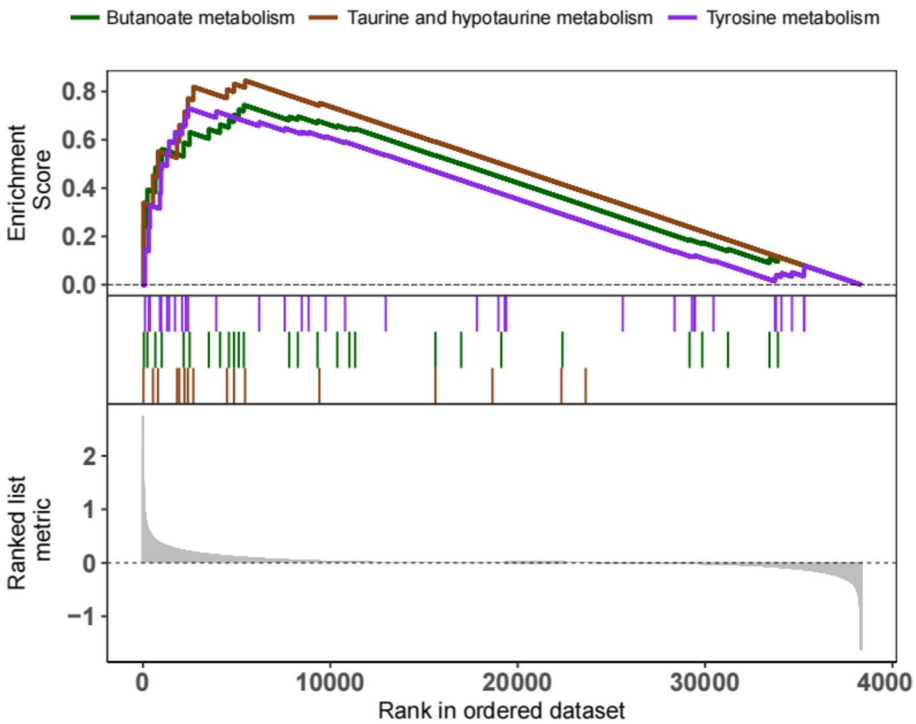

Fig. 8 GSEA enrichment results of SCNN1A

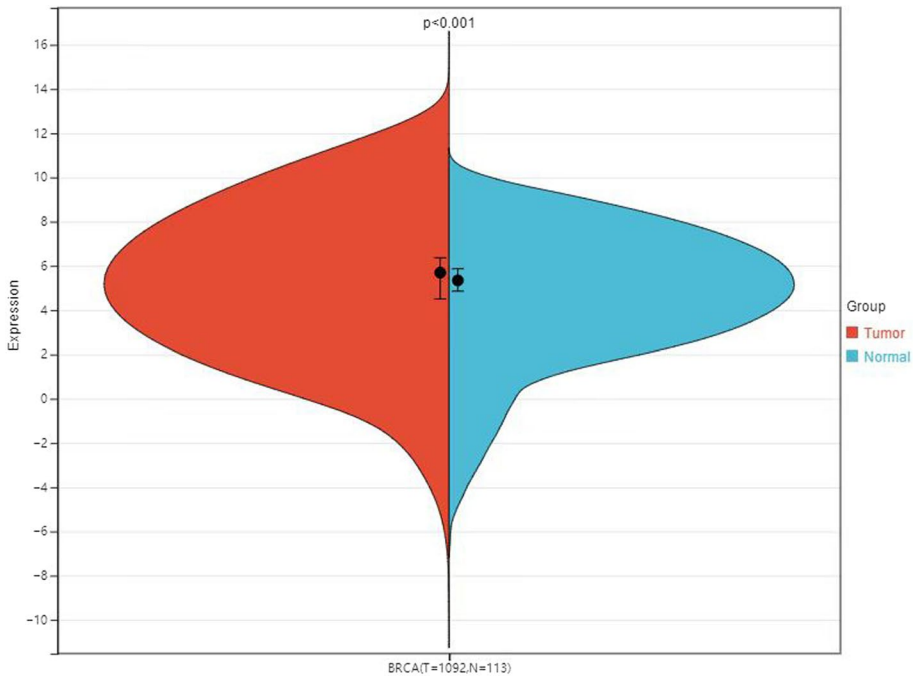

Fig. 9 Expression of SCNN1A in breast cancer tissues

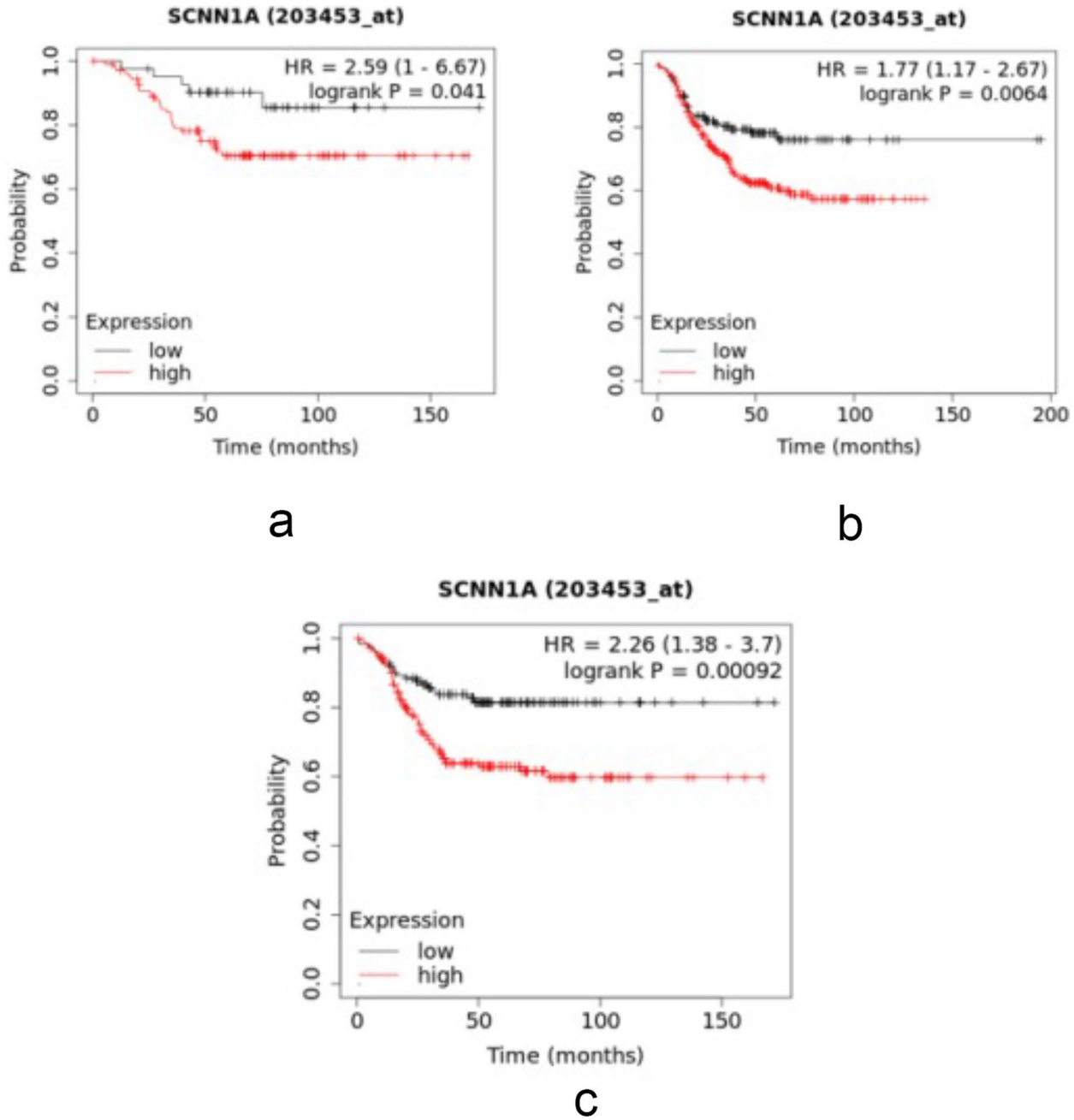

Fig. 10 SCNN1A survival prognosis in triple-negative breast cancer, (a) is OS, (b) is RFS, and (c) is DMFS

of SGK1, thus extending its half-life and augmenting its steady-state expression. Moreover, the increase of Na^+ influx through ENaC accelerates Na^+-H^+ exchange, raising H^+ concentration in the tumor microenvironment and promoting its acidification. An acidic tumor microenvironment has been associated with enhanced invasive capabilities of tumor cells. Furthermore, it has been suggested that the sodium channel cENaC mediates the inflammatory stress response triggered by IL-17, which may foster tumor proliferation and metastasis.

Some studies have demonstrated that silencing *SCNN1A* inhibits the proliferation, migration, and EMT in pancreatic cancer cells [16, 17]. Furthermore, in vitro studies indicated that both HOXD9 and SCNN1A exhibited high expression in pancreatic cancer tissues and cells. The downregulation of these genes was associated with a reduction in cell proliferation, migration, and EMT

Table 1 Clinical data parameter table of triple-negative breast cancer

Clinicopathological features	Frequency
Age	
≤ 60	155
> 60	128
Histological grade	
G1	15
G2	145
G3	123
Tumor size	
T1	51
T2	192
T3	37
T4	3
Lymph node status	
N0	123
N1	112
N2	32
N3	16
Clinical stage	
I	21
II	173
III	89
Ki-67 expression	
< 30%	64
≥ 30%	219
Her-2 status	
Her-2 negative	101
Low expression of Her-2	182

[18]. According to our database analysis, *HOXD9* is predicted to be a transcription factor of *SCNN1A*, and the silencing of *HOXD9* correspondingly reduced *SCNN1A* expression, suggesting a positive transcriptional correlation between *HOXD9* and *SCNN1A* [19]. Moreover, it has been found that *SCNN1A* can form a positive feedback loop with *HOXD9*, thereby continuously enhancing its oncogenic effects and aggravating cancer progression. *HOXD9*, a homeobox gene, is implicated in the pathogenesis of several malignancies, including ovarian and cervical cancers [20]. It promotes the growth, invasion, and metastasis of gastric cancer cells through transcriptionally activating the RUN and FYVE domain-containing protein 2. Furthermore, in TNBC cells and tissues, the low expression of miR-205 alleviated the inhibition of the HOXD9-Snail1 axis on cell proliferation and chemotherapy resistance. High levels of miR-205 expression and Snail1 knockdown significantly inhibited cell proliferation, indicating a negative correlation between the miRNA levels of miR-205 and the expression of HOXD9 protein in BT-549 cells [21]. Additionally, the *HOXD9* gene can directly transcribe and activate the *Snail1* gene. Consequently, it can be hypothesized that miR-205 may inhibit the inhibitory effect of HOXD9-Snail1 on the proliferation and chemotherapy resistance of TNBC cells and tissues. MicroRNAs (miRNAs) are endogenous, small, non-coding single-stranded RNAs that play crucial roles in various biological processes, including tumorigenesis, proliferation, metastasis, EMT, tumor stem cell maintenance, and drug resistance by targeting mRNA for degradation or translational repression [22]. Specifically, miR-205, located on chromosome 1q32.2, is expressed in

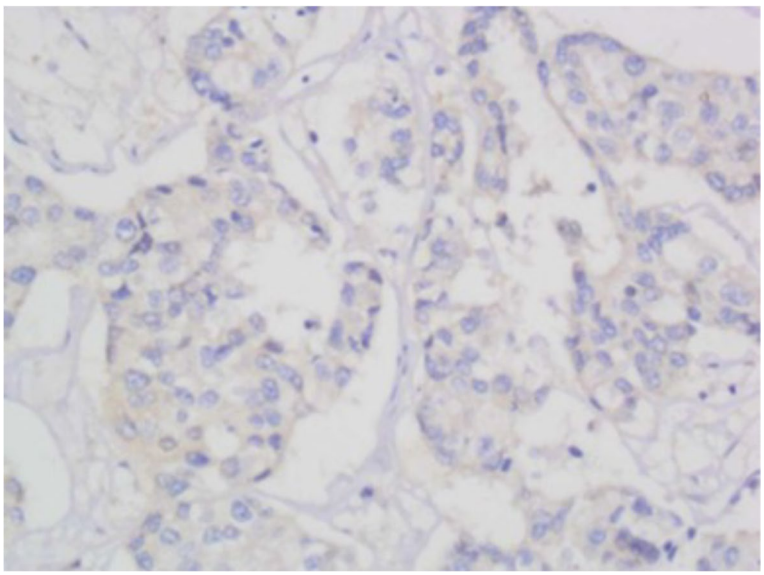

Fig. 11 Low expression of SCNN1A, × 400

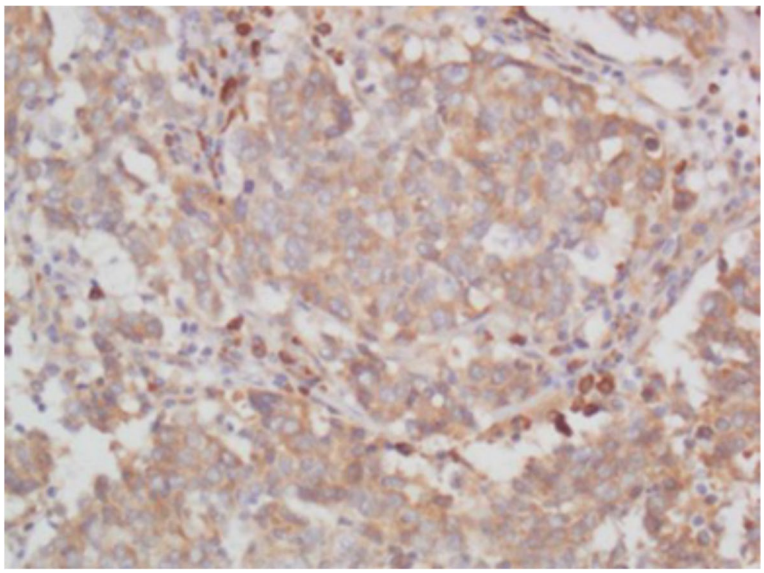

Fig. 12 High expression of SCNN1A, × 400

breast, thymus, and prostate and regulates their development. Among these, miR-205-5p has been shown to be critical in several cancers, particularly exhibiting the lowest expression in TNBC, and this suppressed miR-205-5p expression is associated with high frequency mutation of *TP53* [23]. This study found that a cooperative interaction between miR-200a, miR-200b, and miR-205 significantly inhibits the expression of ZEB1 and SIP1, key transcription factors involved in EMT [24]. With the decrease of ZEB1 and SIP1, we observed a corresponding increase in *E-cadherinm* RNA levels, suggesting that the suppression of these microRNAs is sufficient to induce EMT. EMT is recognized as a critical driver of cancer metastasis and invasion, characterized by enhanced migration ability, invasiveness, resistance to apoptosis, and increased production of extracellular matrix components [25, 26]. These changes reflect the transition from polarized epithelial cells to cells with a more mesenchymal-like phenotype and morphology [27]. Further experiments demonstrated a positive correlation between HOXD9 and SCNN1A transcription. It is postulated that SCNN1A could modulate the expression of miR-205 via the HOXD9-Snail1 axis. This modulation likely occurs through a positive feedback loop between SCNN1A and HOXD9, which may enhance the EMT to promote proliferation and increase chemotherapy resistance in TNBC cells.

GSVA results showed that patients with high expression of *SCNN1A* exhibited enrichment in several key signaling pathways, including ESTROGENRESPONSEEARLY, KRASSIGNALINGDN, XENOBIOTICMETABOLISM. Further, GSEA identified significant involvement of *SCNN1A* in the metabolism of tyrosine, taurine and subtaurine, and butyric acid. These findings are particularly relevant given the increased rates of glycolysis, lipogenesis, and production of volatile organic metabolites observed in the serum of breast cancer patients compared to healthy individuals [28]. Most cancers, including TNBC, demonstrate metabolic plasticity, adapting to highly glycolytic pathways even in the presence of oxygen, a phenomenon known as the Warburg effect [29]. This metabolic reprogramming supports rapid cell growth and proliferation by efficiently converting glucose into lactic acid, which accumulates in the tumor microenvironment, leading to acidification. Activation of tyrosine kinase receptors, such as the fibroblast growth factor receptor (FGFR) and epidermal growth factor receptor (EGFR), have been recognized as a driver of malignancy in numerous cancers. These receptors enhance glycolysis and oxidative phosphorylation, in which FGFR activation facilitates the recovery of lactic acid and the provision of energy for oxidative phosphorylation [30]. Moreover, treatment with epidermal growth factor has been shown to increase the invasive potential of TNBC cells through the tyrosine phosphorylation of β-catenin [31]. The acidic tumor microenvironment resulting from elevated lactic acid levels not only facilitates cancer invasion and metastasis but also contributes to immune escape mechanisms. SCNN1A's involvement in tyrosine metabolism suggests a potential regulatory role in these processes by influencing glycolysis and subsequently the acidity of the tumor environment. However, the full implications of SCNN1A's role in these pathways and its potential impact on tumor progression and immune escape in TNBC require

Table 2 Clinical data correlation between different SCNN1A expression in triple-negative breast cancer

Clinicopathological features	Highly express SCNN1A	Low express SCNN1A	*p*-value
Age			
≤60	84	71	0.848
>60	67	61	
Histological grade			
G1	6	9	0.106
G2	71	74	
G3	74	49	
Tumor size			
T1	18	33	0.037
T2	106	86	
T3	25	12	
T4	2	1	
Lymph node status			
pN0	52	71	0.011
pN1	65	47	
pN2	22	10	
pN3	12	4	
Clinical stage			
I	9	12	0.126
II	87	86	
III	55	34	
Ki-67 expression			
<30%	29	35	0.185
≥30%	122	97	
HER-2 status			
HER-2 negative	54	47	0.922
Low expression of HER-2	97	85	
Neoadjuvant chemotherapy			
pCR	7	16	0.041
non-pCR	16	9	

further investigation and validation through in vitro studies.

The analysis of online databases revealed that *SCNN1A* expression was elevated in breast cancer tissues compared to normal tissues. Importantly, the high expression of SCNN1A was associated with poor prognosis in TNBC, significantly affecting OS, RFS, and DMFS. Further investigations confirmed that elevated SCNN1A expression correlated with advanced T stage ($p=0.037$) and N stage ($p=0.011$), although no significant relationships were observed with age, HER2 status, Ki-67 expression, or histological grade. These findings underscore the importance of SCNN1A as a marker for tumor progression, suggesting that its heightened expression may contribute to the advanced staging of TNBC.

Survival analyses reinforced these observations, demonstrating a notable decline in both OS and DFS in patients exhibiting high SCNN1A expression. The consistency of these results across bioinformatic and clinical datasets highlights the robustness of SCNN1A as a prognostic indicator. Thus, the data strongly suggest that high SCNN1A expression is linked to a decreased OS rate and poorer outcomes in TNBC. Based on these outcomes, we speculated that there is a significant association between the high expression of SCNN1A and adverse prognosis in TNBC. This evidence supports further exploring SCNN1A as a potential therapeutic target for TNBC management.

In this study, we observed that patients with non-pCR to neoadjuvant chemotherapy in TNBC exhibited significantly higher levels of SCNN1A expression compared to those achieving a pCR ($P=0.041$), suggesting that high SCNN1A expression might predict non-pCR outcomes. These findings could guide the development of strategies to increase pCR rates through targeted interventions in SCNN1A pathways. However, given the limited number of TNBC cases undergoing neoadjuvant chemotherapy

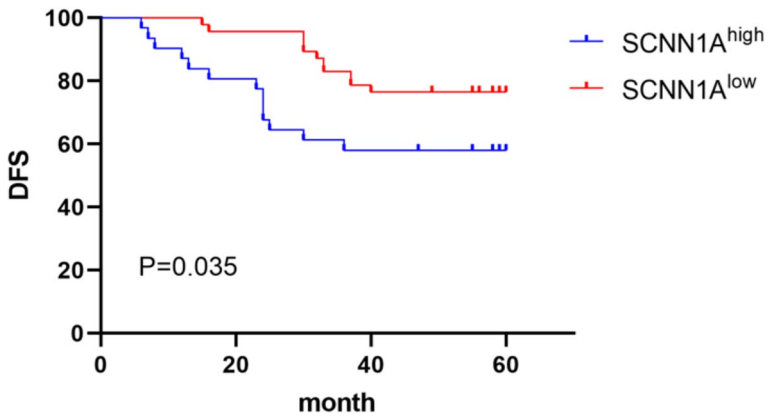

Fig. 13 5-year DFS in different SCNN1A expression populations

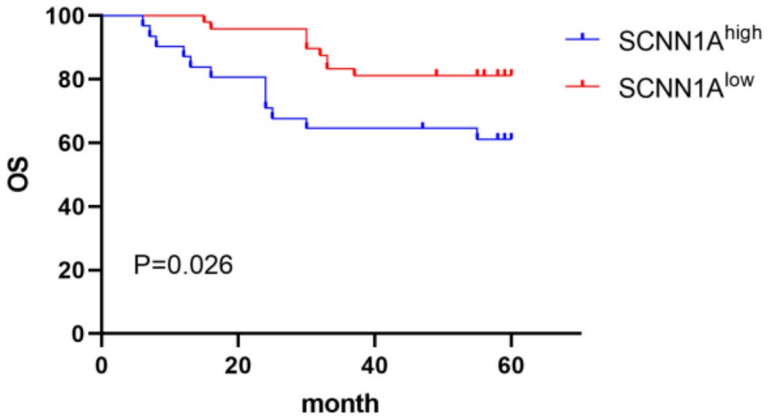

Fig. 14 5-year OS in different SCNN1A expression populations

in our dataset, further validation with a larger cohort is essential to confirm these conclusions.

Neoadjuvant chemotherapy has emerged as a cornerstone in the treatment of triple-negative breast cancer (TNBC), particularly for its ability to reduce tumor burden and improve surgical outcomes. This study focuses on the clinically challenging population of patients who fail to achieve a pathological complete response (non-pCR), utilizing bioinformatics analyses to identify *SCNN1A* as a potential therapeutic target. Further validation using clinical and pathological data demonstrated that differential expression of *SCNN1A* significantly influences patient prognosis and the efficacy of neoadjuvant therapy. These findings suggest that *SCNN1A* may serve as a promising target for the development of novel TNBC therapies.

However, this study has certain limitations. The relatively small sample size of patients receiving neoadjuvant treatment limits the generalizability of the findings, underscoring the need for larger-scale studies to confirm the results. Furthermore, as this represents the initial exploration of *SCNN1A* by our research group, subsequent investigations are required to validate its role and elucidate the underlying mechanisms through in vitro and in vivo experiments. These efforts will be critical in establishing a robust foundation for translational research and clinical application. Ongoing related experiments are expected to further advance our understanding, and updates in this area are highly anticipated.

Abbreviations

pcr	Pathological complete response
TNBC	Triple-negative breast cancer
OS	Overall survival
DFS	Disease-free survival
ER	Estrogen receptor
PR	Progesterone receptor
HER2	Human epidermal growth factor receptor 2
NGS	Next-generation sequencing
non-Pcr	Non-pathological complete response
PPI	Protein–protein interaction
SVM	Support vector machine
SVM-RFE	SVM-Recursive Feature Elimination
GSVA	Gene set difference analysis
MSigDB	Molecular Signatures Database
RFS	Recurrence-free survival
DMFS	Distant metastasis-free survival
ENaC	Epithelial sodium channel
DSS	Disease-specific survival
EMT	Epithelial-mesenchymal transition
MiRNAs	MicroRNAs
FGFR	Fibroblast growth factor receptor
EGFR	Epidermal growth factor receptor

Acknowledgements
Not applicable.

Authors' contributions
Conception and design: JQ, XJ. Administrative support: JQ. Provision of study materials or patients: XJ, YG, TS, YM. Collection and assembly of data: XJ, YG, TS, YZ, YM. Data analysis and interpretation: XJ, QX, FY, LZ. Manuscript writing: All authors. Final approval of manuscript: All authors.

Funding
This study was supported by Key Projects of the Department of Education of Anhui Province (No. 2023AH051980, No. 2022AH051479), Clinical research Special Fund of WU JIEPING Medical Foundation (No. 320.6750.2022–19-79), Open project of Anhui Province Key Laboratory of Cancer Translational Medicine (No. KFDX202203).

Data availability
The datasets used and/or analysed during the current study are available from the corresponding author on reasonable request.

Declarations

Ethics approval and consent to participate
All procedures performed in studies involving human participants were in accordance with the ethical standards of the institutional and/or national research committee and with the 1964 Helsinki Declaration and its later amendments or comparable ethical standards. The study was approved by the Ethics Committee of Bengbu Medical University (2023YJS024). Informed consent was obtained from all individual participants included in the study.

Consent for publication
Informed consent was obtained from all individual participants included in the study.

Competing interests
The authors declare no competing interests.

Author details
[1]Anhui Medical University, Hefei, Anhui, China. [2]Department of Surgical Oncology, The First Affiliated Hospital of Bengbu Medical University, No.287, Changhuai Road, Bengbu, Anhui 233000, China. [3]Bengbu Medical University, Bengbu, Anhui, China. [4]Anhui Province Key Laboratory of Cancer Translational Medicine, Bengbu Medical University, Bengbu, Anhui, China. [5]Department of Pathology, The First Affiliated Hospital of Bengbu Medical University, Bengbu, Anhui, China. [6]Department of Pathology, Bengbu Medical University, Bengbu, China.

Received: 25 September 2024 Accepted: 30 January 2025
Published online: 26 April 2025

References

1. Chen W, Zheng R, Baade PD, et al. Cancer statistics in China, 2015[J]. CA: A Cancer J Clin. 2016;66(2):115–32.
2. Denkert C, Liedtke C, Tutt A, et al. Molecular alterations in triple-negative breast cancer—the road to new treatment strategies[J]. The Lancet. 2017;389(10087):2430–42.
3. Ferlay J, Soerjomataram I, Dikshit R, et al. Cancer incidence and mortality worldwide: sources, methods and major patterns in GLOBOCAN 2012[J]. Int J Cancer. 2015;136(5):E359–86.
4. de Moraes FCA, Souza MEC, Sano VKT, et al. Association of tumor-infiltrating lymphocytes with clinical outcomes in patients with triple-negative breast cancer receiving neoadjuvant chemotherapy: a systematic review and meta-analysis. Clin Transl Oncol. 2025;27(3):974–87.
5. Wei L, Wang H. SCNN1A Overexpression Correlates with Poor Prognosis and Immune Infiltrates in Ovarian Cancer[J]. Int J Gen Med. 2022;15:1743–63.
6. Chang J, Hu X, Nan J, et al. HOXD9-induced SCNN1A upregulation promotes pancreatic cancer cell proliferation, migration and predicts prognosis by regulating epithelial-mesenchymal transformation[J]. Mol Med Rep. 2021;24(5):819.
7. Zhang JB, Song W, Wang YY, et al. Study on correlation between PKIB and pAkt expression in breast cancer tissues[J]. Eur Rev Med Pharmacol Sci. 2017;21(6):1264–9.
8. Mitsiades CS, Mitsiades N, Koutsilieris M. The Akt pathway: molecular targets for anti-cancer drug development[J]. Curr Cancer Drug Targets. 2004;4(3):235–56.
9. Wilson-Edell KA, Yevtushenko MA, Rothschild DE, et al. mTORC1/C2 and pan-HDAC inhibitors synergistically impair breast cancer growth by convergent AKT and polysome inhibiting mechanisms[J]. Breast Cancer Res Treat. 2014;144(2):287–98.
10. Perez-Tenorio G, Stal O. Activation of AKT/PKB in breast cancer predicts a worse outcome among endocrine treated patients[J]. Br J Cancer. 2002;86(4):540–5.
11. Qi D, He J, Wang D, et al. 17β-estradiol suppresses lipopolysaccharide-induced acute lung injury through PI3K/Akt/SGK1 mediated up-regulation of epithelial sodium channel (ENaC) in vivo and in vitro[J]. Respir Res. 2014;15(1):159.
12. Warrington JP, Coleman K, Skaggs C, et al. Heme oxygenase-1 promotes migration and beta-epithelial Na+ channel expression in cytotrophoblasts and ischemic placentas[J]. Am J Physiol Regul Integr Comp Physiol. 2014;306(9):R641–6.
13. Wang L, Liu Y, Wang H, et al. Epoxyeicosatrienoic acids attenuating hypotonic-induced apoptosis of IMCD cells via gamma-ENaC inhibition[J]. PLoS ONE. 2014;9(4): e94400.
14. Geng Y, Zhao S, Jia Y, et al. miR-95 promotes osteosarcoma growth by targeting SCNN1A[J]. Oncol Rep. 2020;43(5):1429–36.
15. Wu L, Ling ZH, Wang H, et al. Upregulation of SCNN1A promotes cell proliferation, migration, and predicts poor prognosis in ovarian cancer through regulating epithelial-mesenchymal transformation[J]. Cancer Biother Radiopharm. 2019;34(10):642–9.
16. Soundararajan R, Wang J, Melters D, et al. Glucocorticoid-induced Leucine zipper 1 stimulates the epithelial sodium channel by regulating serum- and glucocorticoid-induced kinase 1 stability and subcellular localization[J]. J Biol Chem. 2010;285(51):39905–13.
17. Gupta SC, Singh R, Asters M, et al. Regulation of breast tumorigenesis through acid sensors[J]. Oncogene. 2016;35(31):4102–11.
18. Pernia O, Sastre-Perona A, Rodriguez-Antolin C, et al. A novel role for the tumor suppressor gene ITF2 in tumorigenesis and chemotherapy response[J]. Cancers (Basel). 2020;12(4):786.
19. Hirao N, Iwata T, Tanaka K, et al. Transcription factor homeobox D9 is involved in the malignant phenotype of cervical cancer through direct binding to the human papillomavirus oncogene promoter[J]. Gynecol Oncol. 2019;155(2):340–8.
20. Zhu H, Dai W, Li J, et al. HOXD9 promotes the growth, invasion and metastasis of gastric cancer cells by transcriptional activation of RUFY3[J]. J Exp Clin Cancer Res. 2019;38(1):412.
21. Xiao Y, Humphries B, Yang C, et al. MiR-205 dysregulations in breast cancer: the complexity and opportunities[J]. Noncoding RNA. 2019;5(4):53.
22. Hayes J, Peruzzi PP, Lawler S. MicroRNAs in cancer: biomarkers, functions and therapy[J]. Trends Mol Med. 2014;20(8):460–9.
23. Vosgha H, Salajegheh A, Smith RA, et al. The important roles of miR-205 in normal physiology, cancers and as a potential therapeutic target[J]. Curr Cancer Drug Targets. 2014;14(7):621–37.
24. Gregory PA, Bert AG, Paterson EL, et al. The miR-200 family and miR-205 regulate epithelial to mesenchymal transition by targeting ZEB1 and SIP1[J]. Nat Cell Biol. 2008;10(5):593–601.
25. Chaffer CL, Weinberg RA. A perspective on cancer cell metastasis[J]. Science. 2011;331(6024):1559–64.
26. Said NA, Simpson KJ, Williams ED. Strategies and challenges for systematically mapping biologically significant molecular pathways regulating carcinoma epithelial-mesenchymal transition[J]. Cells Tissues Organs. 2013;197(6):424–34.
27. Kalluri R, Weinberg RA. The basics of epithelial-mesenchymal transition[J]. J Clin Invest. 2009;119(6):1420–8.
28. Hadi NI, Jamal Q, Iqbal A, et al. Serum metabolomic profiles for breast cancer diagnosis, grading and staging by gas chromatography-mass spectrometry[J]. Scient Rep. 2017;7(1):1715.
29. Naik A, Decock J. Lactate Metabolism and Immune Modulation in Breast Cancer: A Focused Review on Triple Negative Breast Tumors[J]. Front Oncol. 2020;10: 598626.
30. Jin N, Bi A, Lan X, et al. Identification of metabolic vulnerabilities of receptor tyrosine kinases-driven cancer[J]. Nat Commun. 2019;10(1):2701.
31. Liu Q, He L, Li S, et al. HOMER3 facilitates growth factor-mediated β-Catenin tyrosine phosphorylation and activation to promote metastasis in triple negative breast cancer[J]. J Hematol Oncol. 2021;14(1):6.

Publisher's Note